Inorganic Chemistry

Article

pubs.acs.org/IC

Long-Range Intramolecular Electronic Communication in Bis(ferrocenylethynyl) Complexes Incorporating Conjugated Heterocyclic Spacers: Synthesis, Crystallography, and Electrochemistry

Hakikulla H. Shah,[†] Rayya A. Al-Balushi,[†] Mohammed K. Al-Suti,[†] Muhammad S. Khan,*[,†] Christopher H. Woodall,[‡] Kieran C. Molloy,[‡] Paul R. Raithby,*[,‡] Thomas P. Robinson,[‡] Sara E. C. Dale,[‡] and Frank Marken*[,‡]

[†]Department of Chemistry, Sultan Qaboos University, P.O. Box 36, Al-Khodh 123, Sultanate of Oman

[‡]Department of Chemistry, University of Bath, Bath BA2 7AY, U.K.

Supporting Information

ABSTRACT: A new series of bis(ferrocenylethynyl) complexes, **3**−**7**, and a mono(ferrocenylethynyl) complex, **8**, have been synthesized incorporating conjugated heterocyclic spacer groups, with the ethynyl group facilitating an effective long-range intramolecular interaction. The complexes were characterized by NMR, IR, and UV−vis spectroscopy as well as X-ray crystallography. The redox properties of these complexes were investigated using cyclic voltammetry and spectroelectrochemistry. Although there is a large separation of ∼14 Å between the two redox centers, $\Delta E_{1/2}$ values in this series of complexes ranged from 50 to 110 mV. The appearance of intervalance charge-transfer bands in the UV−vis−near-IR region for the monocationic complexes further confirmed effective intramolecular electronic communication. Computational studies are presented that show the degree of delocalization across the Fc−C≡C−C≡C−Fc (Fc = $C_5H_5FeC_5H_4$) highest occupied molecular orbital.

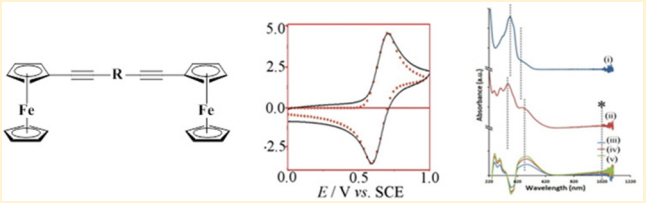

INTRODUCTION

There is considerable contemporary interest in metal-containing polymers in which metal centers are linked by conjugated moieties because these have the potential for facile electron transfer between metals; such species are potential molecular wires, with application in the downscaling of diverse electronic devices.[1−15] Ferrocene-based materials have been central to this research because the complexes are often synthetically robust, show well-defined redox chemistry, and readily support mixed-valence systems.[16−22] In particular, a wide range of ferrocene moieties linked by conjugated spacers such as alkenes,[16,23−27] alkynes,[28] and/or aromatic rings[29−32] have been synthesized and their properties reported. We have a long-standing interest in this general area, and in particular the synthesis and characterization of oligomeric platinum[33−36] and gold[37−40] species linked by alkynes, because these serve as model systems for long-chain polymers. In this paper, we turn our attention to related systems in which ferrocene groups are linked by alkyne/heterocyclic spacers, combining synthesis, crystallography, and spectroelectrochemical studies. Several previous studies have reported alkyne-bridged mixed-valence bis-ferrocene complexes[16,41−50] as well as structural studies of ferrocene groups linked by alkynes and/or oligothiophenes, fluorenes, or similar heterocycles.[31,51−53]

We have synthesized a new series of bis(ferrocenylethynyl) complexes, **3**−**7**, and a mono(ferrocenylethynyl) complex, **8**, incorporating novel heterocyclic spacer groups. Heterocyclic spacer groups, quinoline and benzothiadiazole, have been utilized for complexes **3** and **4**, respectively (Scheme 1). These spacers have been fruitfully used as such and in substituted forms for the development of sensors, taking advantage of the conjugated framework.[54−60] Heterocyclic spacers such as phenyl-substituted thieno[3,4-*b*]pyrazine have shown to be excellent precursors for the production of low-band-gap conjugated polymers[61−63] and have been utilized for the synthesis of complexes **5** and **6**. Similarly, fused thiophenes show better conjugation than their non-fused analogues[64] and thus are used for the synthesis of complexes **7** and **8**. Combining the conjugation properties of the spacers and connecting them to a terminal ferrocene via a rigid rod such as an alkyne should enhance the electronic communication between the two metal centers.

Herein we report the synthesis, characterization, and electrochemical studies of complexes **2**−**8** along with X-ray crystallographic studies of complexes **2**, **4**−**6**, and **8**. The effect of the different spacer groups on the redox properties of the

Received: November 14, 2012

   dx.doi.org/10.1021/ic3024887 | *Inorg. Chem.* XXXX, XXX, XXX−XXX

Scheme 1. Synthesis of Bis(ferrocenylethynyl) Complexes 2−7 and Mono(ferrocenylethynyl) Complex 8

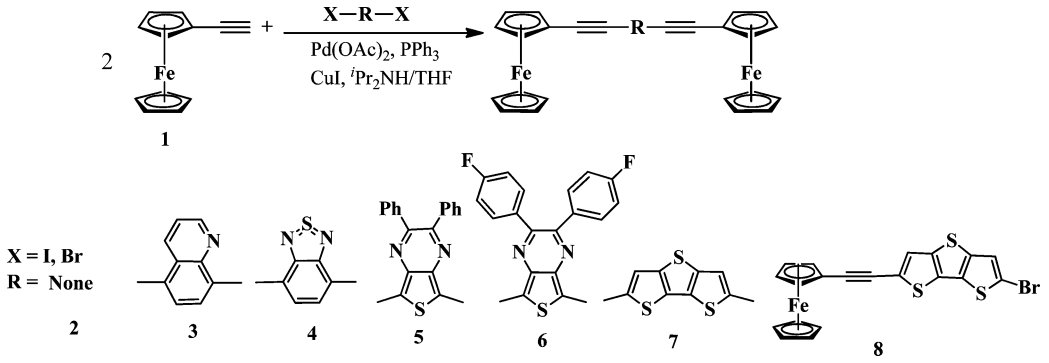

ferrocene is investigated by cyclic voltammetry (CV). The signatures of the monocationic species formed during the long-range intramolecular interaction of the ferrocene units are studied by spectroelectrochemistry. Pure spectra for the monocations are established with the help of spectral deconvolution. Interaction parameters such as the ferrocene-to-ferrocene distance, the separation of the ferrocene reversible potentials, and the features of the intervalence charge-transfer (IVCT) band are discussed.

EXPERIMENTAL SECTION

All reactions were carried out under an inert atmosphere using Schlenk techniques. Solvents were predried and distilled from appropriate drying agents. All chemicals, unless otherwise stated, were obtained from commercial sources and used as received. Preparative thin-layer chromatography was performed on 0.7 mm silica plates. The key starting material, ethynylferrocene, was synthesized by adaptation of a literature method.[25,65,66] The NMR spectra were recorded on a Bruker AM-400 spectrometer in $CDCl_3$. The ^1H NMR spectra were referenced to solvent resonances. IR spectra were recorded as CH_2Cl_2 solutions, in a NaCl cell, on a Nicolet-Impact 400D FT-IR spectrometer amd mass spectrometry (MS) spectra on a Kratos MS 890 spectrometer by electron impact and fast atom bombardment (FAB) techniques. Microanalyses were performed in the Department of Chemistry, University of Bath, Bath, U.K. Computations were performed on the University of Bath's High Performance Computing Facility. Column chromatography was performed on either Kieselgel 60 (230−400 mesh) silica gel or alumina (Brockman grade II−III).

Synthesis. *Ethynylferrocene*[65] ***(1)***. Acetylferrocene (2.14 g, 10 mmol) and triphenylphosphine (10.48 g, 40 mmol) in anhydrous acetonitrile (20 mL) at 0 °C under an argon atmosphere were added to 3.08 g (20 mmol) of tetrachlormethane in one portion. The mixture was warmed to room temperature. Stirring was continued for 45 min, and then 5 mL of distilled water was added to the solution. The mixture was extracted with ether (50 mL × 3), washed with brine, and then dried over anhydrous magnesium sulfate ($MgSO_4$). Solvent was evaporated, and the residue was dissolved in dichloromethane and filtered through a plug of alumina. After removal of the solvent under reduced pressure, a red crystalline intermediate compound was obtained in 85% yield (2.4 g). A total of 1.68 g (6 mmol) of this intermediate compound in 10 mL of dry THF at 0 °C was added to 8 mL (12 mmol) of *n*-BuLi (1.5 M in THF) under rigorous stirring for 10 min. The reaction mixture was warmed to room temperature, and stirring was continued for 15 min followed by hydrolysis with 10 mL of distilled water and stirring for another 10 min. The mixture was extracted with ether (50 mL × 3) and the combined organic layer was dried over $MgSO_4$. After filtration through a plug of alumina and removal of solvent under reduced pressure, the title compound **1** was obtained as a red crystalline solid in 93% yield (1.1 g). IR (CH_2Cl_2): 2110 [ν(C≡C)], 3301 cm^{-1} [ν(C≡CH)]. ^1H NMR (300 MHz, $CDCl_3$): δ 4.21 (s, 5H), 4.19 (t, 2H), 4.47 (t, 2H), 2.71 (s, 1H). FABMS: m/z 211 (M^+). Anal. Calcd for $C_{12}H_{10}Fe$: C, 68.62; H, 4.80. Found: C, 68.53; H, 4.86.

Fc−C≡C−C≡C−Fc ***(2)***. Ethynylferrocene (0.105 g, 0.50 mmol) and diisopropylamine (5 mL) were mixed with catalytic amounts of $Pd(OAc)_2$ (2 mg), CuI (2 mg), and PPh_3 (5 mg). The mixture was allowed to reflux for 15 h under aerobic conditions, after which all volatile components were removed under reduced pressure. The residue was dissolved in CH_2Cl_2 and chromatographed through a silica column using hexane/CH_2Cl_2 (1:1, v/v) as the eluent. The title compound was obtained as a dark-red powder in 95% yield (0.20 g). IR (CH_2Cl_2): 2148 cm^{-1} [ν(C≡C)]. ^1H NMR (300 MHz, $CDCl_3$): δ 3.94 (t, 4H, J = 1.7 Hz, Cp), 4.13 (s, 10H, Cp), 4.46 (t, 4H, J = 1.9 Hz, Cp). FABMS: m/z 419 (M^+). Anal. Calcd for $C_{24}H_{18}Fe_2$: C, 68.95; H, 4.34. Found: C, 68.99; H, 4.29.

Fc−C≡C−R−C≡C−Fc ***(3;*** *R = Quinoline-5,8-diyl)*. Under an argon atmosphere, a solution of ethynylferrocene (0.23 g, 1.1 mmol) and 5,8-diiodoquinoline[67] (0.14 g, 0.5 mmol) in diisopropylamine (15 mL) was mixed with catalytic amounts of $Pd(OAc)_2$ (3 mg), CuI (3 mg), and PPh_3 (10 mg). The mixture was allowed to reflux for 24 h, after which all volatile components were removed under reduced pressure. The residue was dissolved in CH_2Cl_2 and chromatographed through a silica column using hexane/CH_2Cl_2 (2:1, v/v) as the eluent. The title compound was obtained as a dark-red power in 53% yield (0.29 g). IR (CH_2Cl_2): 2188 cm^{-1} [ν(C≡C)]. ^1H NMR (300 MHz, $CDCl_3$): δ 4.11 (pseudo-t, 4H, Cp), 4.31 (s, 10H, Cp), 4.62 (pseudo-t, 4H, Cp), 6.94 (dd, 1H, J = 12.1 Hz, spacer), 7.58 (d, 1H, J = 7.5 Hz, spacer), 7.84 (d, 1H, J = 7.9 Hz, spacer), 8.77 (d, 1H, J = 8.3 Hz, spacer), 8.92 (dd, 1H, J = 6.0 Hz, spacer). FABMS: m/z 546 (M^+). Anal. Calc for $C_{33}H_{23}Fe_2N$: C, 72.89; H, 4.25. Found: C, 72.98; H, 4.29.

Fc−C≡C−R−C≡C−Fc ***(4;*** *R = Benzothiadiazole-4,7-diyl)*. The title bis(ferrocenylethynyl) compound was prepared by following a procedure similar to that described above for **3** using ethynylferrocene (0.23 g, 1.1 mmol) and 4,7-dibromobenzothiadiazole[67] (0.14 g, 0.5 mmol), giving a brown solid in 82% yield (0.45 g). IR (CH_2Cl_2): 2184 cm^{-1} [ν(C≡C)]. ^1H NMR (300 MHz, $CDCl_3$): δ 4.04 (t, 4H, J = 3.4 Hz, Cp), 4.26 (s, 10H, Cp), 4.59 (pseudo-t, 4H, J = 3.8 Hz, Cp), 7.30 (d, 2H, J = 7.5 Hz, spacer). FABMS: m/z 553 (M^+). Anal. Calcd for $C_{30}H_{20}Fe_2N_2S$: C, 65.25; H, 3.65. Found: C, 65.31; H, 3.71.

Fc−C≡C−R−C≡C−Fc ***(5;*** *R = Diphenylthienopyrazine-5,7-diyl)*. The title bis(ferrocenylethynyl) compound was prepared by a procedure similar to that described for **3** using ethynylferrocene (0.23 g, 1.1 mmol) and 5,7-dibromodiphenylthienopyrazine[68] (0.22 g, 0.5 mmol) to obtain a dark-violet powder in 72% yield (0.51 g). IR (CH_2Cl_2): 2199 cm^{-1} [ν(C≡C)]. ^1H NMR (300 MHz, $CDCl_3$): δ 4.04 (pseudo-t, 4H, J = 3.4 Hz, Cp), 4.26 (s, 10H, Cp), 4.59 (pseudo-t, 4H, J = 3.8 Hz, Cp), 7.40 (m, 2H, J = 4.9 Hz, spacer), 7.60−7.63 (m, 8H, spacer). FABMS: m/z 705 (M^+). Anal. Calcd for $C_{42}H_{28}Fe_2N_2S$: C, 71.61; H, 4.01. Found: C, 71.68; H, 4.06.

Fc−C≡C−R−C≡C−Fc ***(6;*** *R = Difluorodiphenylthienopyrazine-5,7-diyl)*. The title bis(ferrocenylethynyl) compound was prepared by a procedure similar to that described for **3** using ethynylferrocene (0.23 g, 1.1 mmol) and 5,7-dibromo(difluorodiphenyl)-thienopyrazine[68] (0.24 g, 0.5 mmol) to obtain a dark-violet powder

dx.doi.org/10.1021/ic3024887 | *Inorg. Chem.* XXXX, XXX, XXX−XXX

Table 1. Crystallographic Data for 4−6 and 8

	4	5	6	8
empirical formula	$C_{30}H_{20}Fe_2N_2S$	$C_{42}H_{28}Fe_2N_2S$	$C_{42}H_{26}F_2Fe_2N_2S$	$C_{20}H_{11}BrFeS_3$
fw	552.24	704.42	740.41	483.23
cryst syst	monoclinic	triclinic	triclinic	triclinic
space group	$C2/c$	$P\bar{1}$	$P\bar{1}$	$P\bar{1}$
a (Å)	30.6586(3)	7.6536(5)	7.4305(5)	7.867(5)
b (Å)	9.8566(1)	12.7415(7)	13.2951(6)	10.000(5)
c (Å)	21.6227(3)	16.5787(11)	16.4962(10)	11.548(5)
α (deg)		100.757(5)	82.729(4)	77.054(5)
β (deg)	134.389(1)	97.360(6)	85.045(5)	86.042(5)
γ (deg)		92.718(5).	80.538(5)	87.945(5)
volume (Å^3)	4669.35(9)	1571.00(17)	1590.97(16)	883.1(8)
Z	8	2	2	2
ρ_{calc} (Mg m^{-3})	1.571	1.489	1.546	1.817
μ(Mo Kα) (mm^{-1})	1.355	1.025	1.025	3.470
F(000)	2256	724	756	480
cryst size (mm)	0.20 × 0.16 × 0.16	0.4 × 0.2 × 0.05	0.30 × 0.30 × 0.10	0.3 × 0.2 × 0.1
θ range (deg)	4.14−25.35	2.81−26.37	2.79−24.71	3.06−29.61
reflns collected	38948	13087	14712	15957
indep reflns [R(int)]	4258 [0.0431]	6388 [0.0603]	5432 [0.0599]	4434 [0.0450]
max, min transmn	0.879, 0.805	1.000, 0.873	1.000, 0.882	1.000, 0.758
GOF on F^2	1.155	0.981	1.102	0.955
final R1, wR2 [$I > 2\sigma(I)$]	0.0368, 0.1040	0.0537, 0.1021	0.0615, 0.1640	0.0422, 0.1020
final R1, wR2 (all data)	0.0452, 0.1092	0.0888, 0.1178	0.0777, 0.1780	0.0684, 0.1165
largest diff peak, hole (e Å^{-3})	0.515, −0.914	0.639, −0.422	1.119, −0.870	0.788, −0.763

in 74% yield (0.55 g). IR (CH_2Cl_2): 2199 cm^{-1} [ν(C≡C)]. ^{1}H NMR (300 MHz, $CDCl_3$): δ 4.04 (pseudo-t, 4H, J = 3.4 Hz, Cp), 4.26 (s, 10H, Cp), 4.59 (pseudo-t, 4H, J = 3.8 Hz, Cp), 6.74 (dd, 4H, J = 8.7 Hz, spacer), 7.33 (dd, 4H, J = 7.3 Hz, spacer). FABMS: m/z 741 (M$^+$). Anal. Calcd for $C_{42}H_{26}F_2Fe_2N_2S$: C, 68.13; H, 3.54. Found: C, 68.78; H, 3.49.

*Fc−C≡C−R−C≡C−Fc (**7**; R = Dithienothiophene-2,5-diyl).* The title bis(ferrocenylethynyl) compound was prepared by a procedure similar to that described for **3** using ethynylferrocene (0.23 g, 1.1 mmol) and 2,5-dibromodithienothiophene[40] (0.16 g, 0.50 mmol) to obtain an orange powder in 68% yield (0.21 g). IR (CH_2Cl_2): 2199 cm^{-1} [ν(C≡C)]. ^{1}H NMR (300 MHz, $CDCl_3$): δ 4.28 (s, 10H, Cp), 4.30 (pseudo-t, 4H, J = 3.4 Hz, Cp), 4.55 (pseudo-t, 4H, J = 3.8 Hz, Cp), 7.39 (s, 2H, spacer). FABMS: m/z 612 (M$^+$). Anal. Calcd for $C_{32}H_{20}Fe_2S_3$: C, 62.76; H, 3.29. Found: C, 62.78; H, 3.19.

*Fc−C≡C−R (**8**; R = 5-Bromodithienothiophene-2-yl).* The title mono(ferrocenylethynyl) compound was prepared by reacting ethynylferrocene (0.23 g, 1.1 mmol) and 2,5-dibromodithienothiophene (0.33 g, 1.0 mmol) at 60 °C for 12 h to obtain orange crystals in 54% yield (0.27 g). IR (CH_2Cl_2): 2199 cm^{-1} [ν(C≡C)]. ^{1}H NMR (300 MHz, $CDCl_3$): δ 3.95 (pseudo-t, 2H, J = 3.8 Hz, Cp), 4.11 (s, 5H, Cp), 4.46 (pseudo-t, 2H, J = 3.8 Hz, Cp), 6.62 (s, 1H, spacer), 7.13 (s, 1H, spacer). FABMS: m/z 483 (M$^+$). Anal. Calcd for $C_{20}H_{11}BrFeS_3$: C, 49.71; H, 2.29. Found: C, 49.78; H, 2.19.

Crystallography. Single-crystal X-ray diffraction experiments were performed at 150(2) K on either an Oxford Diffraction Gemini A Ultra CCD diffractometer (**5**, **6**, and **8**) or an Nonius Kappa CCD diffractometer (**2** and **4**) using monochromatic Mo Kα radiation (λ = 0.71073 Å). For **5**, **6**, and **8**, the sample temperature was controlled using an Oxford Diffraction Cryojet apparatus; *CrysAlis Pro* was used for collecting frames of data, indexing reflections, and determining lattice parameters. For **2** and **4**, temperature control using an Oxford Cryostream device. A multiscan absorption correction was applied in all cases. Structures were solved by direct methods using *SHELXS-86*[69] and refined by full-matric least squares on F^2 using *SHELX-97*.[70] Crystallographic data for all complexes studied can be found in Table 1.

Electrochemistry. Cyclic voltammograms were recorded in a dried glass cell purged with purified argon. A 3-mm-diameter platinum disk electrode was used as the working electrode and a platinum wire served as the counter electrode, while a KCl-saturated calomel electrode (Radiometer ref 401) served as the reference electrode. Under these conditions, the reversible potential for ferrocene is $E_{1/2}$ = 0.527 V. Electrolyte solutions were prepared from dichloroethane (DCE) and [n-Bu_4N][PF_6] (Fluka, dried in oil-pump vacuum) as the supporting electrolyte. The respective organometallic complexes were added at ca. 1 mM concentration. Cyclic voltammograms were recorded using a micro-Autolab III (Ecochemie, The Netherlands). *Digisim*, version 2.0, was employed to simulate CV data.

Spectroelectrochemistry. Spectroelectrochemistry was performed in a home-built optically transparent thin-layer electrolysis (OTTLE) cell by laminating a silver wire (reference), platinum mesh (10 mm × 7.5 mm, working), and platinum wire (auxiliary).[71] The electrode was used in a 0.1-cm-path-length quartz UV−vis cell. Spectra were recorded with reference to the spectrum of the pure solvent by carrying out an initial baseline correction without any potential applied to the solvent-filled cell. UV−vis spectra were then recorded with compounds dissolved in DCE with [n-Bu_4N][PF_6] at different applied potentials. UV−vis data were obtained at a rate of 600 nm min^{-1}. For each measurement, the potential of the OTTLE cell was kept at a constant value and the absorbance spectrum of the solution was recorded between 200 and 1100 nm. Data analysis was based on principle-component analysis programmed in *MATLAB* (version 2010b, Mathworks, Inc.). The equation $\hat{X} = \hat{C}\cdot\hat{S} + \hat{E}$ was used with $\hat{X}$, the experimental spectral matrix at three selected potentials, $\hat{C}$, the concentration coefficients, $\hat{S}$, the pure-component spectra, and $\hat{E}$, the error matrix to be minimized for deconvolution into the pure spectra.[72−74]

RESULTS AND DISCUSSION

Synthesis and Spectroscopic Characterization. The key starting material for the bis(ferrocenylethynyl) compounds, ethynylferrocene (**1**), was prepared in good yield by adaptation of a literature procedure by Luo et al.[65] in preference to other reported synthetic methods for this compound.[25,66] The dibromo/diiodo heteroaromatic precursors for **3**−**7** were prepared as reported previously.[40,67,68,75] The syntheses of **2**−

dx.doi.org/10.1021/ic3024887 | Inorg. Chem. XXXX, XXX, XXX−XXX

8 are shown in Scheme 1. The cross-coupling reactions between ethynylferrocene and dibromo/diiodo heteroaromatic precursors in a 2:1 stoichiometry, in *i*-Pr_2NH/CH_2Cl_2, in the presence of a Pd^{II}/Cu^{I} catalyst readily gave the bis(ferrocenylethynyl) compounds **3**–**7**, while the oxidative homocoupling of **1** under aerobic conditions yielded complex **2**. Complex **8** was synthesized by a 1:1 reaction between **1** and 2,5-dibromodithienothiophene using a lower reaction temperature (60 °C) and a shorter reaction time (12 h). The products of cross-coupling and homocoupling reactions were purified by silica gel column chromatography, giving orange-red crystals (**2**, **4**, and **8**) and dark-blue/black crystals (**5** and **6**) in respectable yields (50–90%). All bis(ferrocenylethynyl) complexes (**2**–**7**) and the monoferrocenylethynyl complex **8** are indefinitely stable to light and air at ambient temperature and were fully characterized by IR and NMR spectroscopy, FAB-MS, as well as by satisfactory elemental analysis.

The IR spectra of the bis(ferrocenylethynyl) complexes show a single, sharp $\nu(C{\equiv}C)$ in the 2200–2010 cm^{-1} range, characteristic of other ethynylferrocenyls[42,43,76] containing aromatic and heteroaromatic spacer groups. The ^1H NMR spectra showed a characteristic pattern of singlet and triplet absorption at ~4 ppm for the unsubstituted and substituted cyclopentadienyl protons, respectively. The aromatic and heteroaromatic spacers gave signals in the 7–8 ppm regions as singlet, doublets, doublet of doublets, and complex multiplets as expected. MS spectra (positive-mode FAB) displayed the presence of molecular ions with characteristic fragmentation patterns for the complexes. The structures of complexes **2**, **4**–**6**, and **8** were confirmed by X-ray crystallography.

The electronic absorption spectra of complexes **2**–**8** were recorded in CH_2Cl_2 (Table 2). Each compound displays three

Table 2. UV–Vis Spectral and Spectroelectrochemical Results for Neutral and Monocationic Forms of 1–8 in DCE

	λ_{max}/nm	
	[complex]	$[complex]^+$
1	267, 399, 514	
2	283, 323, 466	309, 395, 551, 766[a]
3	246, 282, 350, 468	268, 294, 340, 433, 568, 867[a]
4	292, 366, 457	299, 391, 564, 786[a]
5	281, 338	308, 491, 515, 677
6	316, 382	268, 297, 407, 501
7	322, 370, 396, 478	265, 302, 342, 510, 1020[a]
8	261, 363, 466	284, 308, 417, 563, 760[b]

[a]Spectroscopic data for the IVCT band. [b]Spectroscopic data for the MLCT band.

sets of absorption bands. Bands with λ_{max} below 400 nm can be attributed to a π–π^* transition associated with the organic spacer group. A weak absorption band at ~450 nm is assigned to a Fe^{II} d–d transition[15] but is overlapped by the strong, broad higher-energy peak at ~400 nm arising from a π–π^* transition associated with the organic spacer group.

Structural Studies. The structures of **4**–**6** and **8** are shown in Figures 1–4, respectively, along with selected geometric data. Room temperature data for **2** have been reported previously,[45,42] but our low-temperature data are included in Table 3 for a direct comparison across the range of structures at a constant temperature. In **2**, the two ferrocenyl units are linked by a $-C{\equiv}C-C{\equiv}C-$ spacer leading to a Fe···Fe separation of

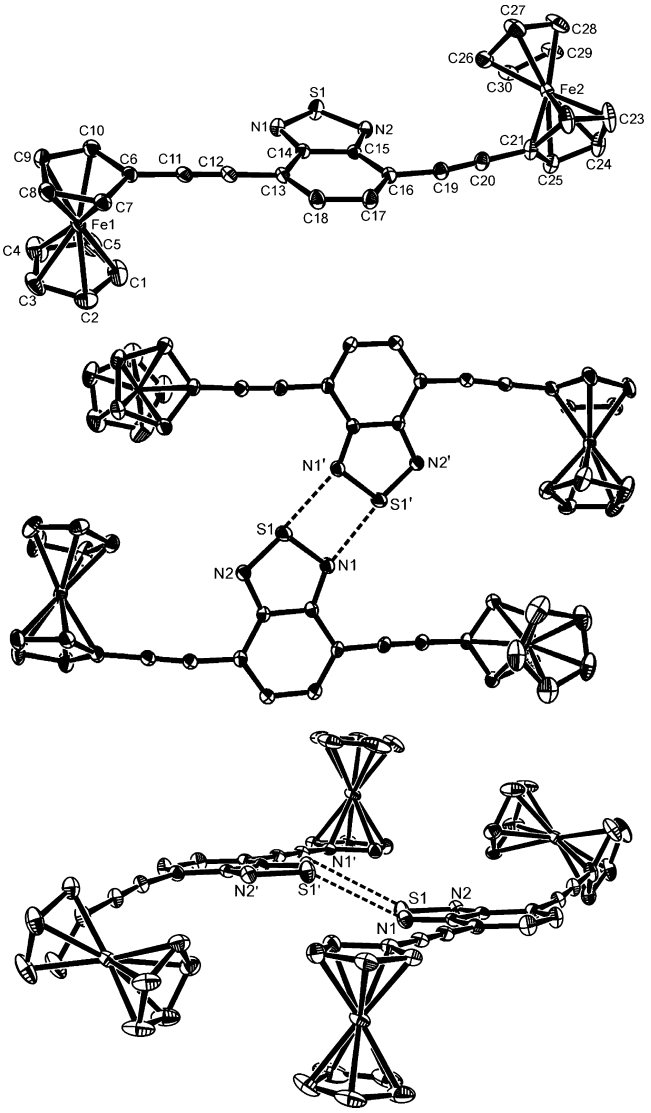

Figure 1. Structure of **4** showing (a, top) the asymmetric unit and labeling scheme used in the text, (b, middle) dimerization via short N···S contacts, and (c, bottom) the offset in heterocycle stacking. Thermal ellipsoids are at the 30% level. Selected geometric data: Fe1–C(1,5) ring centroid 1.6558(13), Fe1–C(6,10) ring centroid 1.6440(11), Fe2–C(21,25) ring centroid 1.6470(15), Fe1–C(26,30) ring centroid 1.6570(15), C6–C11 1.432(3), C11–C12 1.186(3), C12–C13 1.438(3), C16–C19 1.432(3), C17–C18 1.414(4), C19–C20 1.187(3), C20–C21 1.430(4), N1–S1 1.616(2), N2–S1 1.613(2), C14–N1 1.343(3), C14–C15 1.430(3), C15–N2 1.346(3), S1–N1′ 3.098(2) Å; C12–C11–C6 177.4(3), C11–C12–C13 178.1(3), C20–C19–C16 171.1(3), C19–C20–C21 179.5(4)°.

9.5965(5) Å; the two ferrocenyl groups are disposed in an anti manner with respect to each other at the termini of the conjugated alkynes. The C≡C bond is the longest [1.201(3) Å] seen in this study (Table 3) and is accompanied by a C–C single bond between alkynes [1.374(4) Å], which is the shortest observed, although the other structures reported herein have the Fc–C≡C bonded to a heterocycle, not another alkyne [Fc = $(C_5H_5)Fe(C_5H_4)$]. These bond lengths suggest some delocalization along the C≡C–C≡C unit. The $-C{\equiv}C-C{\equiv}C-$ unit is essentially linear, with only minor deviations from ideal bond angles of 180° at the sp C atoms (Table 3); the $-C{\equiv}C-C{\equiv}C-$ torsion angle is −8.7°. The

dx.doi.org/10.1021/ic3024887 | Inorg. Chem. XXXX, XXX, XXX–XXX

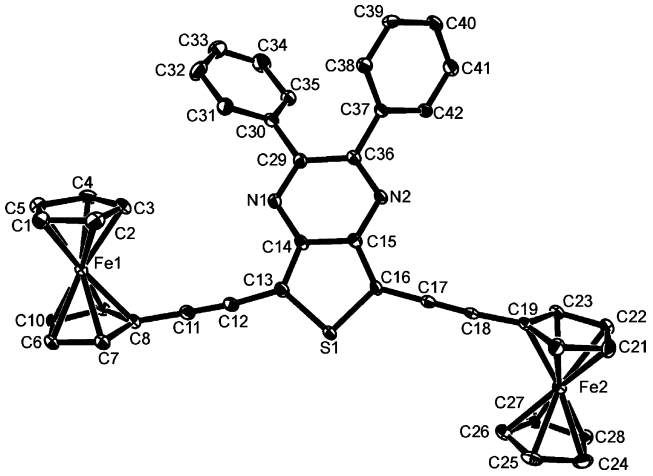

Figure 2. Structure of **5** showing the asymmetric unit and labeling scheme used in the text. Thermal ellipsoids are at the 30% level. Selected geometric data: Fe1−C(1,5) ring centroid 1.6477(19), Fe1−C(6,10) ring centroid 1.6422(18), Fe2−C(19,23) ring centroid 1.6455(18), Fe1−C(24,28) ring centroid 1.6475(18), C8−C11 1.439(5), C11−C12 1.191(5), C12−C13 1.414(5), C16−C17 1.426(5), C17−C18 1.189(4), C18−C19 1.439(5), C16−S1 1.724(3), C13−S1 1.727(4), C14−N1 1.370(4), C14−C15 1.431(4), C15−N2 1.371(4), C15−C16 1.394(5) Å; C12−C11−C8 175.9(4), C11−C12−C13 174.3(4), C18−C17−C16 179.9(4), C17−C18−C19 175.5(4)°.

C_5H_4 unit connected to this latter fragment is close to being coplanar with it [torsion angle between C_5H_4 and C−C≡C = 178.84(17)°], and the exocyclic Fc−C(≡C) bond length [1.428(3) Å], comparable with the C−C bond lengths within the Cp ring, also suggests some degree of multiple-bond character.

In **4**, the two alkynes in **2** are further separated by a benzothiadiazole-4,7-diyl spacer, increasing the Fe···Fe separation to 13.4942(5) Å (Figure 1a). While the exocyclic bond between C_5H_4 and C≡C remains the same as those in **2** [C6−C11 and C21−C20 = 1.432(3) and 1.430(4) Å, respectively], C≡C appears to shorten [1.186(3) and 1.187(3) Å] but just remains within $\pm 3\sigma$ of the analogous bond length in **2**. However, the bonds at the other end of the alkyne [C12−C13 and C16−C19 = 1.438(3) and 1.432(8) Å, respectively] are lengthened with respect to **2**, and collectively the data suggest a more localized C≡C, which retains some possible conjugation with the organometallic fragment but less so with the heterocycle. This asymmetry is also manifested in the angular distortion at C19 [171.1(3)°]. Moreover, the orientation of the two Fc units with respect to each other also differs markedly from that of **2**. While each Fc remains coplanar with C≡C [torsion ∠C8−C7−C6−C11 = −179.9°; torsion ∠C23−C22−C21−C20 = −178.9°], the two Fc units are close to orthogonal to each other [torsion angle between C_5H_4 planes C6−C10 and C21−C25 = 108.74(12)°], implying that any conjugation is with differing components of the π manifold at either end of the molecule. The benzothiadiazole heterocycle is planar and coplanar with the C6−C10 ring of Fc1 but twisted out of conjugation with Fc2. In addition, there is a distinct curvature of the C≡C−Fc2 fragment upward from the plane of the heterocycle (a feature also seen in **6** and **8** but not **5**; see below). This difference may arise from the fact that there are close S···N contacts between pairs of molecules (Figure 1b; S1···N1 = 3.098(2) Å], although the planes of the two heterocycles are offset (Figure 2c).

The structures of **5** (Figure 2) and **6** (Figure 3a) are related to that of **4** but now incorporate a thienopyrazine spacer substituted at the 5 and 6 positions of the pyrazine ring; in **4**, the alkyne is bonded to the six-membered ring, while in **5** and **6**, it is bonded to the smaller ring. The fused five- and six-membered rings common to **4**−**6** have similar dimensions, and although the alkynes are linked differently between the two systems, this has little impact on the Fe···Fe separation [**4**, 13.4942(5) Å; **5**, 13.0742(11) Å; **6**, 13.2918(12) Å]. It should, however, be noted that, in solution, free rotation about the Fc−C(≡C) bond will lead to a variety of Fe···Fe distances. The key bond lengths within the Fc−C≡C−C unit (figure captions and Table 3) are the same within experimental error as those for **4**, but there are differences in the spatial orientation of the Fc units with respect to each other. Thus, in **5**, the two Fc units are anti across the extended −C≡C−(Het)−C≡C moiety (as seen in **2**), while in **6**, they approach orthogonality [torsion angle between C_5H_4 planes C6−C10 and C19−C23 = 80.1(2)°] similar to **4**; this has the effect of making the Fe···Fe separation marginally shorter than that in **6**. The lattice structure of **6** (Figure 3b) shows short F···S contacts [F1···S1 = 3.315(3) Å] and π stacking of heterocycles in a head-to-tail manner with an interplane separation of ca. 4 Å [plane centroid to plane = 3.681(4) Å]. In contrast, there are no close intermolecular contacts of any significance in **5** [shortest, C9−H1···N2 = 2.650 Å], and although pairs of molecules stack with a separation of ca. 4 Å [plane centroid to plane = 4.087(2) Å], the two heterocycles are significantly offset with respect to each other.

The structure of **8** (Figure 4a) has the Fc unit linked via the alkyne to a 5-bromodithienothiophene-2-yl-fused tricycle. The key bond distances and angles (figure captions) are similar to the structures already described (Table 3). The Fc ring is orthogonal to the heterocycle [torsion angle between the C6−C10 ring and the best plane through the heterocycle = 85.21(11)°] so that the organometallic and heterocycle units conjugate with different π components of the alkyne, as seen in **4** and **6**. The lattice of **8** reveals short S···S contacts [S1···S2′ 3.322(4) Å], generating dimers that stack with heterocycles head-to-tail with each other [Figure 4b; plane centroid to plane = 3.469(2) Å]. There is also a visible curvature of the C≡C−Fc moiety away from the plane of the heterocycle, as seen also in **4** and **6**.

Overall, there is little variation in the geometric parameters associated with any putative conjugation across these molecules (Table 3), and, indeed, with similar systems previously reported,[43,44,46,47] save for the fact that data for **2** shows potentially the greatest delocalization of the π-electron density between metal centers. This is supported by the IR data, which show a much lower ν(C≡C) for **2** (2148 cm^{-1}) than the other complexes structurally characterized (2184−2199 cm^{-1}). There are differences in the relative orientations (in the solid state) of the Fc moieties at either end of the molecule, between those that are anti (**2** and **5**) and those that are orthogonal (**4**, **6**, and **8**), although in all of these latter cases, there are significant intermolecular contacts that conceivably cause reorientation of the Fc units to accommodate packing.

Electrochemistry and Spectroelectrochemistry. Cyclic voltammograms for the oxidation of bis(ferrocenylethynyl) complexes **2**−**7** and mono(ferrocenylethynyl) complex **8** in DCE were recorded as a function of the scan rate (20−1000

dx.doi.org/10.1021/ic3024887 | Inorg. Chem. XXXX, XXX, XXX−XXX

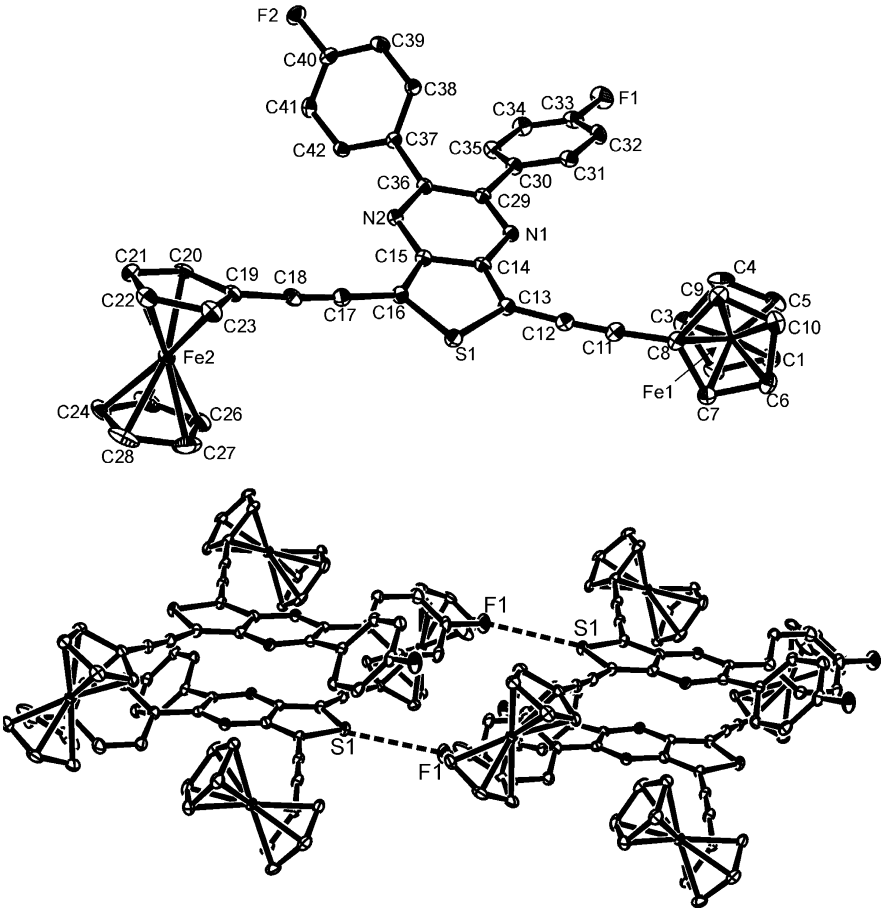

Figure 3. Structure of **6** showing (a, top) the asymmetric unit and labeling scheme used in the text and (b, bottom) dimerization via F···S contacts. Thermal ellipsoids are at the 30% level. Selected geometric data: Fe1−C(1,5) ring centroid 1.646(2), Fe1−C(6,10) ring centroid 1.647(2), Fe2−C(19,23) ring centroid 1.639(2), Fe1−C(24,28) ring centroid 1.645(3), C8−C11 1.431(7), C11−C12 1.192(7), C12−C13 1.406(7), C16−C17 1.425(7), C16−S1 1.717(5), C17−C18 1.190(7), C18−C19 1.429(7), C13−S1 1.721(4), C16−S1 1.717(5), C14−N1 1.368(6), C15−N2 1.356(6), F1···S1′ 3.315(3) Å; C12−C11−C8 176.4(5), C11−C12−C13 175.5(5), C18−C17−C16 176.3(5), C17−C18−C19 176.2(6)°. Symmetry operation: $x, y - 1, z$.

mV s^{-1}) and over a 0−1 V potential range. All complexes were reversibly oxidized as expected for mono- or bis-(ferrocenylethynyl) derivatives connected via conjugated spacers[29,30] (see Figure 5). $E_{1/2}$ values ranging from 610 to 750 mV for the current series (compared to that for ferrocene, $E_{1/2}$ = 0.527 V) indicate the electron-withdrawing nature of the spacers (see Table 4). Two clearly resolved overlapping oxidation waves were observed in the case of complex **2** (Figure 5A) with a separation of ca. $\Delta E_{1/2}$ = 105 mV [here $\Delta E_{1/2} = {E_{1/2}}^{II} - {E_{1/2}}^{I}$) with the midpoint potential $E_{1/2} = 0.5(E_{p,ox} + E_{p,red})$]. This indicates a moderately strong electronic interaction between the two Fe atoms, which is not surprising given the shorter Fe−Fe distance (9.597 Å) and good conjugation in this case.

For complexes **3**−**7**, broadened CV peaks without significant splitting of the midpoint potentials were observed under similar conditions (see Figure 5). This could result from a considerably longer Fe−Fe distance, i.e., ca. ∼14 Å. Several studies have shown that substantial electronic interaction may still occur in cases where conjugated organic spacers are used to link the metal centers. Swager reported that redox matching between the metal and organic components in several transition metal-containing conjugated polymers resulted in enhanced conductivities despite the absence of peak separation in the metal redox waves.[9,77−79]

Some other reports have also shown substantial electronic interactions even in the absence of any observable peak separation. For example, despite small $Ru^{II/III}$ peak separations in the voltammetry, the hybrid metallopolymers bearing bis(2,2′-bipyridyl)ruthenium moieties on a conjugated backbone[80,81] showed electron diffusion coefficients greater than those for comparable non-conjugated materials by an order of magnitude. Broad CV peaks similar to those of complexes **3**−**7** have been reported for ferrocenylethynyl polyynes and oligoynes, and the broadening is attributed to the presence of closely spaced redox processes.[82−84]

To investigate the extent of broadening of the CV peaks in complexes **3**−**7**, the CV features were reproduced by digital simulation with *Digisim* (see Figure 5). Successful simulations of the main features in experimental CVs showed that the broadening in the CV peaks can be reconciled with the presence of two individual, closely spaced, one-electron processes. Figure 5 documents the agreement between the experimental and simulated CVs for the bis(ferrocenylethynyl)

dx.doi.org/10.1021/ic3024887 | *Inorg. Chem.* XXXX, XXX, XXX−XXX

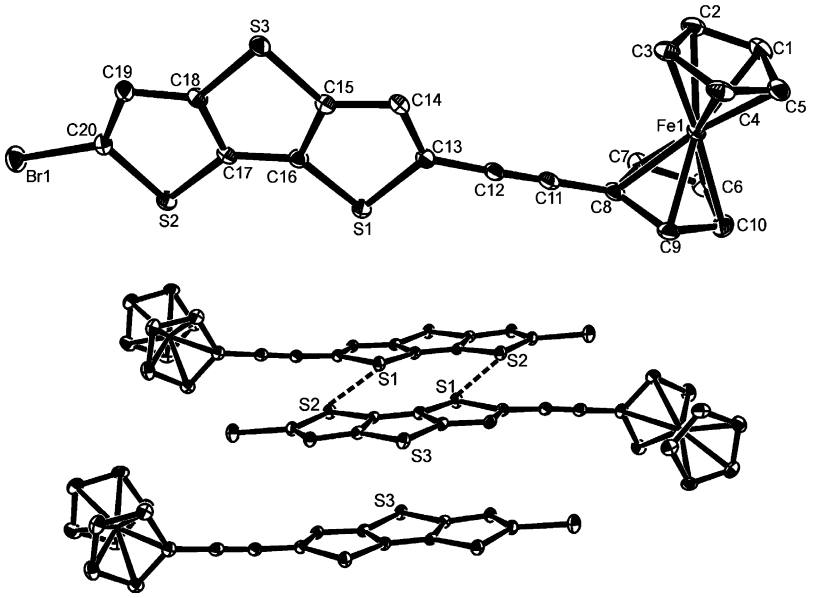

Figure 4. Structure of **8** showing (a, top) the asymmetric unit and labeling scheme used in the text and (b, bottom) dimerization via short S···S contacts. Thermal ellipsoids are at the 30% level. Selected geometric data: Fe1−C(1,5) ring centroid 1.6497(19), Fe1−C(6,10) ring centroid 1.6428(18), C8−C11 1.435(5), C12−C11 1.182(5), C13−C12 1.426(5), S1−C16 1.719(4), S1−C13 1.758(4), S3−C15 1.741(4), S3−C18 1.743(4), S2−C20 1.723(4), S2−C17 1.722(3), Br1−C20 1.867(4), S1···S2′ 3.322(4) Å; C12−C11−C8 179.7(4), C11−C12−C13 176.6(4)°. Symmetry operation: $1 - x$, $1 - y$, $1 - z$.

Table 3. Comparison of Key Structural Data for the Fc−C≡C−C Unit of 2, 4−6, and 8

	C≡C (Å)	Fc−C(≡C) (Å)	(C≡)C−C (Å)	∠Fc−C≡C−C (deg)	Fe···Fe (Å)
2[a]	1.201(3)	1.428(3)	1.374(4)	178.7(2), 179.8(3)	9.5965(5)
4	1.186(3)	1.432(3)	1.438(3)	177.4(3), 178.1(3)	13.4942(5)
	1.187(3)	1.430(4)	1.432(8)	171.1(3), 179.4(4)	
5	1.191(5)	1.439(5)	1.414(5)	175.9(4), 174.3(4)	13.0742(11)
	1.189(4)	1.439(5)	1.426(5)	179.9(4), 175.5(4)	
6	1.192(7)	1.431(7)	1.406(7)	176.4(5), 175.5(5)	13.2918(12)
	1.190(7)	1.429(7)	1.425(7)	176.3(5), 176.2(6)	
8	1.182(5)	1.435(5)	1.426(5)	179.7(4), 176.6(4)	

[a]Data collected at 150 K as part of this work. Room temperature data are given in refs 45 and 51.

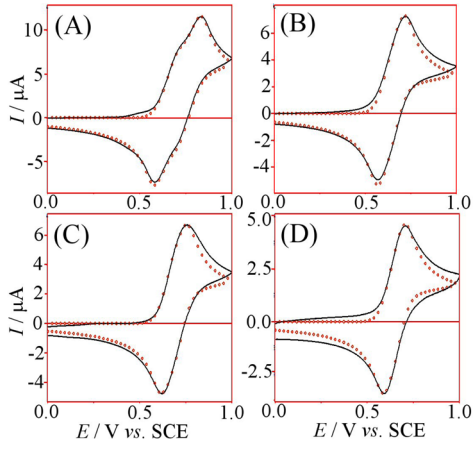

Figure 5. Simulation curves (red circles) matched with cyclic voltammograms (black line) for bis(ferrocenylethynyl) complexes **2** (A), **3** (B), **5** (C), and **7** (D) in DCE at 25 °C with 0.1 M [*n*-Bu_4N]PF_6 as the supporting electrolyte and at scan rate 100 mV s^{-1}.

Table 4. Electrochemical Data in Millivolts versus SCE for Complexes 2−8 Obtained from Voltammograms in DCE Containing 0.1 M [*n*-Bu_4N]PF_6 at ca. 20 °C (Errors Are Estimated)

complex	$E_{1/2}^{I}$ ± 5 (mV)	$E_{1/2}^{II}$ ± 5 (mV)[a]	$\Delta E_{1/2}$ ± 5 (mV)	IVCT bandwidth at half-height (cm^{-1})	ε_{IVCT} (L mol^{-1} cm^{-1})
2	645	750	105	2364	212
3	612	667	55	2512	478
4	630	740[b]	110	1988	542
5	650	720	70	[c]	[c]
6	650	730[b]	80	[c]	[c]
7	620	672	52	2843[d]	441[d]
8	610	[e]	[e]	[e]	[e]

[a]Values obtained from digital simulation of the cyclic voltammograms. [b]Estimated values from digital simulation in the presence of an unknown impurity. [c]Due to the limited spectral window, the IVCT band could not be located. [d]IVCT band, in part, outside the analysis range; thus, a bandwidth estimate is reported. [e]Mono-(ferrocenylethynyl) complex.

complexes **2**, **3**, **5**, and **7**. The simulation CVs for complexes **4** and **6** (not shown here) had minor additional, and so far unidentified, impurity oxidation peaks.

A recent report demonstrated significant electronic communication in bis(ferrocenyl) complexes separated by electron-withdrawing spacers and having Fe−Fe distances of <8 Å.[16]

dx.doi.org/10.1021/ic3024887 | *Inorg. Chem.* XXXX, XXX, XXX−XXX

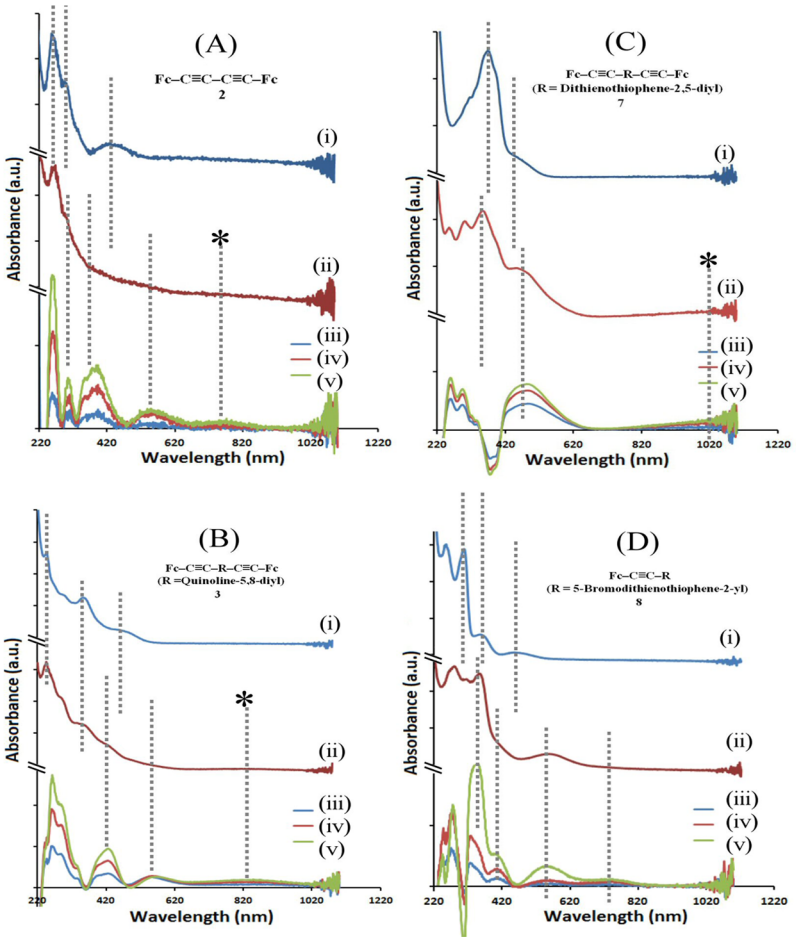

Figure 6. UV–vis spectra of complexes **2**, **3**, **7**, and **8** in a DCE solution at different potentials applied in OTTLE cells with $[n\text{-}Bu_4N]PF_6$ as the supporting electrolyte [data for the neutral spectra (i), the monocation (ii), and difference spectra (iii–v) are shown]: (A) **2** with (i) neutral, (ii) 650 mV, and (iii–v) 540, 650, and 710 mV; (B) **3** with (i) neutral, (ii) 620 mV, and (iii–v) 580, 620, and 660 mV ;(C) **7** with (i) neutral, (ii) 630 mV,and (iii–v) 600, 630, and 660 mV; (D) **8** with (i) neutral, (ii) 650 mV, and (iii–v) 620, 650, and 690 mV, respectively.

Interestingly, **2**, which has a Fe–Fe distance of 9.597 Å, and **4**, which has a Fe–Fe distance of 13.494 Å, still exhibit similar $\Delta E_{1/2}$, i.e., 105 and 110 mV, respectively, which is not too dissimilar compared to values for *p*-diferrocenylbenzene.[28] The electron-withdrawing nature of the spacer could have an impact on the net conjugation effect, overriding the Fe–Fe distance effect in this particular comparison. Other bimetallic complexes supported by bis(NHC) (NHC = N-heterocyclic carbene) ligands exhibit weaker interactions ($\Delta E_{1/2}$ = 42–80 mV) despite having direct metal–NHC connections and metal–metal distances of less than 11 Å.[82] $\Delta E_{1/2}$ values of 80 and 70 mV were found for **6** and **5**, respectively, although they have Fe–Fe distances similar to that of complex **4**. This can be explained by the fact that the connecting unit in **5** and **6** is substituted thiophene, which is less conjugated than the substituted benzene unit in complex **4**. Recent reports suggest that electron-withdrawing spacers play an important role in the communication of the terminal ferrocene units.[16,85,86] This is reflected in the $\Delta E_{1/2}$ values for complexes **2**–**7**, which range from 50 to 110 mV. While there is no clear relation between the half-wave potential splitting and the strength of the electronic interaction between coupled redox sites,[87,88] the values of $\Delta E_{1/2}$ (Table 4) suggest that they belong to class II according to the Robin and Day classification scheme[89] with modest coupling.

UV–vis spectra were recorded at different applied potentials for complexes **2**–**8**. An initial spectrum was collected in an OTTLE cell without applying any potential, and a series of spectra were then collected by gradually changing the applied potential. The spectra collected in the proximity of the $E_{1/2}^{I}$ value were used for deconvolution to obtain a pure spectrum of the monocationic species (see the Experimental Section). Figure 6 summarizes neutral and monocation spectra and shows difference spectra where weak bands are more clearly resolved. The oxidation of complexes **2**–**8** resulted in strong absorption bands with λ_{max} in the range 260–310 nm assigned to a π–π^* transition in the organic spacer groups. The shoulder at ~440–570 nm in these spectra is due to a Cp → Fe^{III} ligand-to-metal charge-transfer (LMCT) band and has been reported for related compounds.[90,91] The broad absorption bands close to the near-IR (NIR) region can be assigned as IVCT bands.

Upon oxidation of **2** to $\mathbf{2}^+$, the intensity of the low-energy MLCT bands at 395 nm decreases, while the intensity of the higher-energy, predominantly π–π^* band increases. In addition, new broad bands at 551 and ~766 nm appear in the spectrum. The NIR band was assigned as an IVCT transition. The IVCT nature was confirmed because this band disappears upon further oxidation by increasing the potential.[92] Similar observations were found for **3**, where during the spectroelectrochemical oxidation of **3** to $\mathbf{3}^+$ the intensity of the

dx.doi.org/10.1021/ic3024887 | *Inorg. Chem.* XXXX, XXX, XXX–XXX

low-energy MLCT bands at 484 nm decreases, while the intensity of the higher-energy $\pi-\pi^*$ band increases; in addition, new bands at 568 and 867 nm appear in the spectrum. The former band might consist of overlapping MLCT and LMCT transitions. The NIR was assigned as an IVCT transition (Figure 6B). The spectroelectrochemical oxidation of complexes **4**−**7** is consistent with the data collected for **2** and **3** (Table 1); for **5** and **6**, the IVCT bands could not be observed in the spectral window. In Figure 6C(i),(ii), the spectra of complexes **7** and $\mathbf{7}^+$ show subtle shifts in the visible absorption, where there is an increase in the intensity of the $\pi-\pi^*$ band at higher energy and a red shift of the initial MLCT band at 466 nm to a new band at 510 nm. The IVCT band here appears at much longer wavelength, ∼1020 nm, and continues outside the analysis range. The LMCT band at 510 nm for complex **7** can be compared with the LMCT band at 563 nm of complex **8**, i.e., a mono(ferrocenylethynyl) complex with similar spacer group (Figure 6D). This band in **8** is further shifted to lower energy compared to **7** because of the inductive effect of the terminal bromine. Further, **8** shows a MLCT band at ∼760 nm.

It is interesting to compare optical and electrochemical data. A stronger intramolecular interaction should correspond to an increased $\Delta E_{1/2}$, but also the IVCT band oscillator strength given by $4.6 \times 10^{-9}\varepsilon_{max}\Delta\nu_{1/2}$ (ε_{max} is the extinction coefficient maximum, and $\Delta\nu_{1/2}$ is the half-width of the IVCT band[93]) should increase. However, this predicted trend cannot be confirmed here. As the $\Delta E_{1/2}$ value increases, the IVCT bandwidth appears to decrease, which suggests a lower oscillator strength at assumed similar extinction maxima. For example, in the series of complexes **3**, **2**, and **4**, the $\Delta E_{1/2}$ values increase 50, 105, and 110 mV, but the IVCT bandwidth at half-height decreases as 2512, 2364, and 1988 cm^{-1}, respectively. Clearly structural effects introduced by the spacer system and additional configurational changes in solution could add complexity and limit the applicability of the $\Delta E_{1/2}$ oscillator strength correlation. Further experimental work, in particular taking into account solvent polarity effects, will be desirable.

Computational Studies. IR and structural analysis indicated that complex **2** may potentially have the greatest delocalization of the π-electron density between metal centers. The electrochemistry results ($\Delta E_{1/2}$ = 105 mV) for complex **2** comparable to complex **4** ($\Delta E_{1/2}$ = 110 mV) motivated us to select complexes **2** and **4** to conduct computational studies to gain better insight into the intramolecular interaction processes. We have therefore attempted to model the delocalization computationally using the B3LY[94] hybrid density functional under the *Gaussian09* package[95] for complexes **2** and **4**. The SDD pseudopotential and associated basis set[96] was used for Fe atoms, and the 6-31G(d)[97] basis set was used for all other atoms. Geometry optimizations were performed and frequency calculations were used to confirm that the stationary points were true minima; pictures of the highest occupied molecular orbitals (HOMOs) for **2** and **4** are given in Figure 7. For **2**, the HOMO shows extensive delocalization across the whole molecule, with contributions of 26 (Fe), 11 (C_5H_4), and 23% (C≡C−C≡C) from the contributing fragments. Similarly, the HOMO for **4** (Figure 7, right), although less symmetrical than that for **2**, has contributions of 33, 20 (Fe, Fe), 11, 8 (C_5H_4, C_5H_4). 7, 7 (C≡C, C≡C), and 14% (C_6NSN).

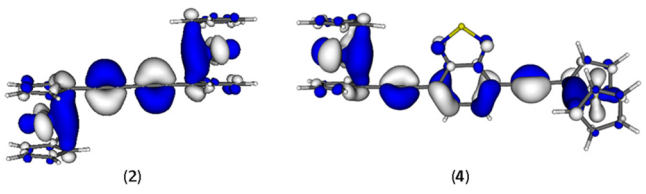

Figure 7. HOMOs of **2** (left) and **4** (right).

CONCLUSION

We have successfully established a synthetic protocol for bis(ferrocenylethynyl) complexes **3**−**7** and mono-(ferrocenylethynyl) complex **8** and characterized these complexes using NMR, IR, mass, and UV−vis spectroscopies. Complexes **4**−**6** and **8** were characterized by X-ray crystallography. The redox properties of these complexes were investigated using a CV approach and digital simulation revealing two one-electron oxidation processes with differences ranging from 50 to 110 mV. Spectroelectrochemistry performed in an OTTLE cell gave a clear indication of the formation of monocationic species. The appearance of IVCT bands for complexes **2**−**4** and **7** further confirms the monocationic species. This work is an example of longer range electronic interaction where the Fe−Fe distance is ∼14 Å and the spacer is electron-withdrawing. Computational studies show that there is significant electron delocalization between iron centers in the HOMOs of both **2** and **4**. It is demonstrated that the conjugated spacer is important in tuning the optical and redox properties of the bis(ferrocenylethynyl) complexes. The results obtained have important implications for the design and synthesis of metal-containing conjugated polyynes and oligoynes.

ASSOCIATED CONTENT

Supporting Information

Crystallographic data for structural analysis (in CIF format). This material is available free of charge via the Internet at http://pubs.acs.org. These have also been deposited with the Cambridge Crystallographic Data Center as CCDC 610675−610679 for **2**, **4**−**6**, and **8**, respectively. Copies of this information may be obtained from the Director, CCDC, 12 Union Road, Cambridge CB21EZ, U.K. (fax +44-1233-336033; e-mail deposit@ccdc.cam.ac.uk, or weblink www.ccdc.cam.ac.uk).

AUTHOR INFORMATION

Corresponding Author

*E-mail: msk@squ.edu.om (M.S.K.), p.r.raithby@bath.ac.uk (P.R.R.), f.marken@bath.ac.uk (F.M.).

Notes

The authors declare no competing financial interest.

ACKNOWLEDGMENTS

We acknowledge the Sultan Qaboos University, Oman, for a research grant and for a research leave to M.S.K. H.H.S. and R.A.A. acknowledge Sultan Qaboos University, Oman, for Ph.D. scholarships. We are grateful to the British Council for a PMI-2 grant (GS 216) that has supported M.S.K., M.K.A., H.H.S., P.R.R. and K.C.M. P.R.R. gratefully acknowledges support from the EPSRC through the award of a Senior Fellowship. We also thank Dr. Dariusz Matoga of Jagiellonian University, Poland, for helpful discussions on some CV data.

REFERENCES

(1) Whittell, G. R.; Hager, M. D.; Schubert, U. S.; Manners, I. *Nat. Mater.* **2011**, *10*, 176.
(2) Burroughes, J. H.; Bradley, D. D. C.; Brown, A. R.; Marks, R. N.; Mackay, K.; Friend, R. H.; Burns, P. L.; Holmes, A. B. *Nature* **1990**, *347*, 539.
(3) Kraft, A.; Grimsdale, A. C.; Holmes, A. B. *Angew. Chem., Int. Ed.* **1998**, *37*, 402.
(4) Montali, A.; Smith, P.; Weder, C. *Synth. Met.* **1998**, *97*, 123.
(5) Tessler, N.; Denton, G. J.; Friend, R. H. *Nature* **1996**, *382*, 695.
(6) Meier, H. *Angew. Chem., Int. Ed.* **1992**, *31*, 1399.
(7) Halls, J. J. M.; Walsh, C. A.; Greenham, N. C.; Marseglia, E. A.; Friend, R. H.; Moratti, S. C.; Holmes, A. B. *Nature* **1995**, *376*, 498.
(8) Köhler, A.; Wittmann, H. F.; Friend, R. H.; Khan, M. S.; Lewis, J. *Synth. Met.* **1994**, *67*, 245.
(9) Köhler, A.; Wittmann, H. F.; Friend, R. H.; Khan, M. S.; Lewis, J. *Synth. Met.* **1996**, *77*, 147.
(10) Swager, T. M. *Acc. Chem. Res.* **1998**, *31*, 201.
(11) Khan, M. S.; Al-Suti, M. K.; Shah, H. H.; Al-Humaimi, S.; Al-Battashi, F. R.; Bjernemose, J. K.; Male, L.; Raithby, P. R.; Zhang, N.; Kohler, A.; Warren, J. E. *Dalton Trans.* **2011**, *40*, 10174.
(12) Ho, C.-L.; Wong, W.-Y. *Coord. Chem. Rev.* **2011**, *255*, 2469.
(13) Wong, W.-Y.; Ho, C.-L. *Acc. Chem. Res.* **2010**, *43*, 1246.
(14) Wong, W.-Y.; Harvey, P. D. *Macromol. Rapid Commun.* **2010**, *31*, 671.
(15) Wong, W.-Y.; Ho, C.-L. *Coord. Chem. Rev.* **2006**, *250*, 2627.
(16) Solntsev, P. V.; Dudkin, S. V.; Sabin, J. R.; Nemykin, V. N. *Organometallics* **2011**, *30*, 3037.
(17) Santi, S.; Orian, L.; Donoli, A.; Bisello, A.; Scapinello, M.; Benetollo, F.; Ganis, P.; Ceccon, A. *Angew. Chem., Int. Ed.* **2008**, *47*, 5331.
(18) Astruc, D.; Ornelas, C.; Ruiz Aranzaes, J. *J. Inorg. Organomet. Polym. Mater.* **2008**, *18*, 4.
(19) Wagner, M. *Angew. Chem., Int. Ed.* **2006**, *45*, 5916.
(20) Barlow, S.; O'Hare, D. *Chem. Rev.* **1997**, *97*, 637.
(21) Kaifer, A. E. *Eur. J. Inorg. Chem.* **2007**, 5015.
(22) Barlow, S. *Inorg. Chem.* **2001**, *40*, 7047.
(23) Debroy, P.; Roy, S. *Coord. Chem. Rev.* **2007**, *251*, 203.
(24) Thomas, K. R. J.; Lin, J. T.; Wen, Y. S. *Organometallics* **2000**, *19*, 1008.
(25) Yin, J.; Yu, G.-A.; Tu, H.; Liu, S. H. *Appl. Organomet. Chem.* **2006**, *20*, 869.
(26) Auger, A.; Swarts, J. C. *Organometallics* **2007**, *26*, 102.
(27) Nemykin, V. N.; Hadt, R. G. *J. Phys. Chem. A* **2010**, *114*, 12062.
(28) Low, P.; Roberts, R.; Cordiner, R.; Hartl, F. *J. Solid State Electrochem.* **2005**, *9*, 717.
(29) Zhu, Y.; Wolf, M. O. *J. Am. Chem. Soc.* **2000**, *122*, 10121.
(30) Diallo, A. K.; Daran, J.-C.; Varret, F.; Ruiz, J.; Astruc, D. *Angew. Chem., Int. Ed.* **2009**, *48*, 3141.
(31) Yuan, Y.-F.; Cardinaels, T.; Lunstroot, K.; Van Hecke, K.; Van Meervelt, L.; Görller-Walrand, C.; Binnemans, K.; Nockemann, P. *Inorg. Chem.* **2007**, *46*, 5302.
(32) Tanaka, Y.; Inagaki, A.; Akita, M. *Chem. Commun.* **2007**, 1169.
(33) Warren, M. R.; Brayshaw, S. K.; Hatcher, L. E.; Johnson, A. L.; Schiffers, S.; Warren, A. J.; Teat, S. J.; Warren, J. E.; Woodall, C. H.; Raithby, P. R. *Dalton Trans.* **2012**, *41*, 13173.
(34) Saha, R.; Qaium, M. A.; Debnath, D.; Younus, M.; Chawdhury, N.; Sultana, N.; Kociok-Kohn, G.; Ooi, L.-l.; Raithby, P. R.; Kijima, M. *Dalton Trans.* **2005**, 2760.
(35) Wilson, J. S.; Chawdhury, N.; Al-Mandhary, M. R. A.; Younus, M.; Khan, M. S.; Raithby, P. R.; Köhler, A.; Friend, R. H. *J. Am. Chem. Soc.* **2001**, *123*, 9412.
(36) Markwell, R. D.; Butler, I. S.; Kakkar, A. K.; Khan, M. S.; Al-Zakwani, Z. H.; Lewis, J. *Organometallics* **1996**, *15*, 2331.
(37) de la Riva, H.; Nieuwhuyzen, M.; Mendicute Fierro, C.; Raithby, P. R.; Male, L.; Lagunas, M. C. *Inorg. Chem.* **2006**, *45*, 1418.
(38) Pintado-Alba, A.; de la Riva, H.; Nieuwhuyzen, M.; Bautista, D.; Raithby, P. R.; Sparkes, H. A.; Teat, S. J.; Lopez-de-Luzuriaga, J. M.; Lagunas, M. C. *Dalton Trans.* **2004**, 3459.
(39) Li, P.; Ahrens, B.; Bond, A. D.; Davies, J. E.; Koentjoro, O. F.; Raithby, P. R.; Teat, S. J. *Dalton Trans.* **2008**, 1635.
(40) Li, P.; Ahrens, B.; Feeder, N.; Raithby, P. R.; Teat, S. J.; Khan, M. S. *Dalton Trans.* **2005**, 874.
(41) Cuffe, L.; Hudson, R. D. A.; Gallagher, J. F.; Jennings, S.; McAdam, C. J.; Connelly, R. B. T.; Manning, A. R.; Robinson, B. H.; Simpson, J. *Organometallics* **2005**, *24*, 2051.
(42) Thomas, K. R. J.; Lin, J. T.; Wen, Y. S. *Organometallics* **2000**, *19*, 1008.
(43) Chawdhury, N.; Long, N. J.; Mahon, M. F.; Ooi, L.-l.; Raithby, P. R.; Rooke, S.; White, A. J. P.; Williams, D. J.; Younus, M. *J. Organomet. Chem.* **2004**, *689*, 840.
(44) Wong, W.-Y.; Ho, K.-Y.; Choi, K.-H. *J. Organomet. Chem.* **2003**, *670*, 17.
(45) Rodriguez, J.-G.; Oñate, A.; Martin-Villamil, R. M.; Fonseca, I. *J. Organomet. Chem.* **1996**, *513*, 71.
(46) Wong, W.-Y.; Ho, K.-Y.; Ho, S.-L.; Lin, Z. *J. Organomet. Chem.* **2003**, *683*, 341.
(47) Wong, W.-Y.; Lu, G.-L.; Ng, K.-F.; Wong, C.-K.; Choi, K.-H. *J. Organomet. Chem.* **2001**, *637*−*639*, 159.
(48) Wong, W.-Y.; Lu, G.-L.; Choi, K.-H.; Guo, Y.-H. *J. Organomet. Chem.* **2005**, *690*, 177.
(49) Wong, W.-Y.; Lu, G.-L.; Ng, K.-F.; Choi, K.-H.; Lin, Z. *J. Chem. Soc., Dalton Trans.* **2001**, *0*, 3250.
(50) Bruce, M. I.; Low, P. J.; Hartl, F.; Humphrey, P. A.; de Montigny, F.; Jevric, M.; Lapinte, C.; Perkins, G. J.; Roberts, R. L.; Skelton, B. W.; White, A. H. *Organometallics* **2005**, *24*, 5241.
(51) Tanaka, Y.; Ishisaka, T.; Inagaki, A.; Koike, T.; Lapinte, C.; Akita, M. *Chem.—Eur. J.* **2010**, *16*, 4762.
(52) McAdam, C. J.; Cameron, S. A.; Hanton, L. R.; Manning, A. R.; Moratti, S. C.; Simpson, J. *CrystEngComm* **2012**, *14*, 4369.
(53) Morisaki, Y.; Murakami, T.; Chujo, Y. *J. Inorg. Organomet. Polym.* **2009**, *19*, 104.
(54) Wang, Q.; Wong, W.-Y. *Polym. Chem.* **2011**, *2*, 432.
(55) Dai, F.-R.; Zhan, H.-M.; Liu, Q.; Fu, Y.-Y.; Li, J.-H.; Wang, Q.-W.; Xie, Z.; Wang, L.; Yan, F.; Wong, W.-Y. *Chem.—Eur. J.* **2012**, *18*, 1502.
(56) Wang, X.-Z.; Wang, Q.; Yan, L.; Wong, W.-Y.; Cheung, K.-Y.; Ng, A.; Djurišić, A. B.; Chan, W.-K. *Macromol. Rapid Commun.* **2010**, *31*, 861.
(57) He, G.; Yan, N.; Cui, H.; Liu, T.; Ding, L.; Fang, Y. *Macromolecules* **2011**, *44*, 7096.
(58) Saito, N.; Kanbara, T.; Nakamura, Y.; Yamamoto, T.; Kubota, K. *Macromolecules* **1994**, *27*, 756.
(59) Tokoro, Y.; Nagai, A.; Kokado, K.; Chujo, Y. *Macromolecules* **2009**, *42*, 2988.
(60) Wong, W.-Y.; Wang, X.-Z.; He, Z.; Djurisic, A. B.; Yip, C.-T.; Cheung, K.-Y.; Wang, H.; Mak, C. S. K.; Chan, W.-K. *Nat. Mater.* **2007**, *6*, 521.
(61) Nietfeld, J. P.; Schwiderski, R. L.; Gonnella, T. P.; Rasmussen, S. C. *J. Org. Chem.* **2011**, *76*, 6383.
(62) Kenning, D. D.; Mitchell, K. A.; Calhoun, T. R.; Funfar, M. R.; Sattler, D. J.; Rasmussen, S. C. *J. Org. Chem.* **2002**, *67*, 9073.
(63) Zhou, E.; Cong, J.; Yamakawa, S.; Wei, Q.; Nakamura, M.; Tajima, K.; Yang, C.; Hashimoto, K. *Macromolecules* **2010**, *43*, 2873.
(64) Roncali, J. *Chem. Rev.* **1992**, *92*, 711.
(65) Luo, S.-J.; Liu, Y.-H.; Liu, C.-M.; Liang, Y.-M.; Ma, Y.-X. *Synth. Commun.* **2000**, *30*, 1569.
(66) Rosenblum, M.; Brawn, N.; Papenmeier, J.; Applebaum, M. *J. Organomet. Chem.* **1966**, *6*, 173.
(67) Khan, M. S.; Al-Suti, M. K.; Al-Mandhary, M. R. A.; Ahrens, B.; Bjernemose, J. K.; Mahon, M. F.; Male, L.; Raithby, P. R.; Friend, R. H.; Kohler, A.; Wilson, J. S. *Dalton Trans.* **2003**, 65.
(68) Younus, M.; Köhler, A.; Cron, S.; Chawdhury, N.; Al-Mandhary, M. R. A.; Khan, M. S.; Lewis, J.; Long, N. J.; Friend, R. H.; Raithby, P. R. *Angew. Chem., Int. Ed.* **1998**, *37*, 3036.
(69) Sheldrick, G. M. *Acta Crystallogr., Sect. A: Found. Crystallogr.* **1990**, *46*, 467.
(70) Sheldrick, G. M. *Acta Crystallogr., Sect. A* **2008**, *64*, 112.

dx.doi.org/10.1021/ic3024887 | *Inorg. Chem.* XXXX, XXX, XXX−XXX

(71) Neudeck, A.; Kress, L. *J. Electroanal. Chem.* **1997**, *437*, 141.
(72) Shamsipur, M.; Hemmateenejad, B.; Babaei, A.; Faraj-Sharabiani, L. *J. Electroanal. Chem.* **2004**, *570*, 227.
(73) Yamada, Y.; Mizutani, J.; Kurihara, M.; Nishihara, H. *J. Organomet. Chem.* **2001**, *637*−*639*, 80.
(74) Keesey, R. L.; Ryan, M. D. *Anal. Chem.* **1999**, *71*, 1744.
(75) Khan, M. S.; Al-Suti, M. K.; Al-Mandhary, M. R. A.; Ahrens, B.; Bjernemose, J. K.; Mahon, M. F.; Male, L.; Raithby, P. R.; Friend, R. H.; Kohler, A.; Wilson, J. S. *Dalton Trans.* **2003**, 65.
(76) Huang, P.; Jin, B.; Liu, P.; Cheng, L.; Cheng, W.; Zhang, S. *J. Organomet. Chem.* **2012**, *697*, 57.
(77) Zhu, S. S.; Carroll, P. J.; Swager, T. M. *J. Am. Chem. Soc.* **1996**, *118*, 8713.
(78) Zhu, S. S.; Swager, T. M. *J. Am. Chem. Soc.* **1997**, *119*, 12568.
(79) Kingsborough, R. P.; Swager, T. M. *Adv. Mater.* **1998**, *10*, 1100.
(80) Cameron, C. G.; Pickup, P. G. *J. Am. Chem. Soc.* **1999**, *121*, 11773.
(81) Cameron, C. G.; Pickup, P. G. *Chem. Commun.* **1997**, 303.
(82) Mercs, L.; Neels, A.; Albrecht, M. *Dalton Trans.* **2008**, 5570.
(83) Reddinger, J. L.; Reynolds, J. R. *Macromolecules* **1997**, *30*, 673.
(84) Plenio, H.; Hermann, J.; Sehring, A. *Chem.—Eur. J.* **2000**, *6*, 1820.
(85) Chen, Y. J.; Pan, D. S.; Chiu, C. F.; Su, J. X.; Lin, S. J.; Kwan, K. S. *Inorg. Chem.* **2000**, *39*, 953.
(86) Chung, M.-C.; Gu, X.; Etzenhouser, B. A.; Spuches, A. M.; Rye, P. T.; Seetharaman, S. K.; Rose, D. J.; Zubieta, J.; Sponsler, M. B. *Organometallics* **2003**, *22*, 3485.
(87) Mücke, P.; Linseis, M.; Záliš, S.; Winter, R. F. *Inorg. Chim. Acta* **2011**, *374*, 36.
(88) Maurer, J.; Winter, R.; Sarkar, B.; Záliš, S. *J. Solid State Electrochem.* **2005**, *9*, 738.
(89) Robin, M. B.; Day, P. *Adv. Inorg. Chem.* **1968**, *10*, 247.
(90) Zhu, Y. B.; Wolf, M. O. *Chem. Mater.* **1999**, *11*, 2995.
(91) Sohn, Y. S.; Hendrickson, D. N.; Gray, H. B. *J. Am. Chem. Soc.* **1971**, *93*, 3603.
(92) Levanda, C.; Bechgaard, K.; Cowan, D. O. *J. Org. Chem.* **1976**, *41*, 2700.
(93) Hildebrandt, A.; Schaarschmidt, D.; Claus, R.; Lang, H. *Inorg. Chem.* **2011**, *50*, 10623.
(94) (a) Becke, A. D. *J. Chem. Phys.* **1993**, *98*, 5648. (b) Lee, C. T.; Yang, W. T.; Parr, R. G. *Phys. Rev. B* **1988**, *37*, 785.
(95) Frisch, M. J. et al. *Gaussian09*, revision D.01; Gaussian, Inc.: Wallingford, CT, 2004.
(96) Andrae, D.; Haussermann, U.; Dolg, M.; Stoll, H.; Preuss, H. *Theor. Chim. Acta* **1990**, *77*, 123.
(97) (a) Ditchfield, R.; Hehre, W. J.; Pople, J. A. *J. Chem. Phys.* **1971**, *54*, 724. (b) Hariharan, P. C.; Pople, J. A. *Theor. Chim. Acta* **1973**, *28*, 213.

dx.doi.org/10.1021/ic3024887 | *Inorg. Chem.* XXXX, XXX, XXX−XXX